

Inverse Design Methods for Indoor Ventilation Systems Using CFD-Based Multi-Objective Genetic Algorithm

Zhiqiang (John) Zhai^{1,2*}, Yu Xue¹, Qingyan Chen^{1,3}

¹School of Environmental Science and Engineering, Tianjin University, Tianjin 300072, China

²University of Colorado at Boulder, Boulder, CO, 80309, USA

³School of Mechanical Engineering, Purdue University, IN 47905, USA

*Corresponding email: john.zhai@colorado.edu

Abstract

Conventional designers typically count on thermal equilibrium and require ventilation rates of a space to design ventilation systems for the space. This design, however, may not provide a conformable and healthy micro-environment for each occupant due to the non-uniformity in airflow, temperature and ventilation effectiveness as well as potential conflicts in thermal comfort, indoor air quality (IAQ) and energy consumption. This study proposes two new design methods: the constraint method and the optimization method, by using advanced simulation techniques - computational fluid dynamics (CFD) based multi-objective genetic algorithm (MOGA). Using predicted mean vote (PMV), percentage dissatisfied of draft (PD) and age of air around occupants as the design goals, the simulations predict the performance curves for the three indices that can thus determine the optimal solutions. A simple 2-D office and a 3-D aircraft cabin were evaluated, as demonstrations, which reveal both methods have superior performance in system design. The optimization method provides more accurate results while the constraint method needs less computation efforts.

Keywords: Inverse Modeling, Multi-Objective Genetic Algorithm, Computational Fluid Dynamics, Predicted Mean Vote, Percent Dissatisfied, Age of Air

1. Introduction

Good thermal balance, adequate ventilation rate and energy use efficiency are three important indices for heating, ventilation and air-conditioning (HVAC) system designs. Conventional design will start from the heating and cooling load as well as minimum ventilation rate requirement to determine the appropriate supply conditions of HVAC systems. This approach may not be able to satisfy the comfort and indoor air quality (IAQ) needs for all occupants. This may be attributed to non-uniformity of airflow, temperature and ventilation effectiveness caused by specific HVAC designs. Sometimes, potential conflicts among design goals and implementation approaches can also contribute to the challenges.

Optimization methods have been developed and applied to assist the design of optimal HVAC systems, including the use of advanced tools and optimization algorithms. For instance, Huang and Lam [1] used the genetic algorithm (GA) for automatic tuning of proportional, integral and derivative (PID) controllers in HVAC systems to achieve optimal performance. Wright et al. [2] investigated the application of a multi-objective genetic algorithm (MOGA) search method in identifying optimum pay-off characteristic between the building energy cost and the occupant thermal discomfort. Fong et al. [3] proposed a simulation-optimization approach to resetting suitable operating parameters of HVAC system without scarfing

1 thermal comfort. To predict the non-uniformity of flow and heat (and further thermal comfort
 2 and air quality) in a space, computational fluid dynamics technique is inevitable. Zhou and
 3 Haghghat [4][5] combined the GA, artificial neural network (ANN) and CFD to optimize
 4 ventilation system in office spaces. Their design objective function was constructed to
 5 aggregate and weight several indices (for thermal comfort, IAQ, and ventilation energy usage).
 6 Boithias at al. [6] also proposed a GA-based method to optimize the architecture, training
 7 parameters and inputs of an ANN that is used to predict energy use and indoor discomfort
 8 during building control optimization.

Nomenclature

PMV	predicted mean vote	I_{cl}	thermal resistance of clothing (clo)
M	metabolic heat production (Wm^{-2})	T_u	turbulence intensity (%)
W	external work accomplished (W)	u	velocity in x direction (m s^{-1})
t_a	temperature of ambient air ($^{\circ}\text{C}$)	v	velocity in y direction (m s^{-1})
t_{cl}	temperature of clothing ($^{\circ}\text{C}$)	w	velocity in z direction (m s^{-1})
f_{cl}	clothing area factor	τ	age of air (s)
V	air velocity (ms^{-1})	D	diffusion coefficient ($\text{m}^2 \text{s}^{-1}$)
\bar{t}_r	mean radiation temperature($^{\circ}\text{C}$)	T_{inlet}	temperature of inlet flow($^{\circ}\text{C}$)
h_c	convection heat transfer coefficient ($\text{Wm}^{-2}\text{K}^{-1}$)	V_{inlet}	velocity of inlet flow(ms^{-1})
p_a	water vapor pressure of ambient air (kPa)		
V_{sd}	standard deviation of the velocity measured with an omnidirectional anemometer having a 0.2s time constant		

9
 10 It is widely understood that thermal balance calculation based on perfect mixing assumption
 11 cannot ensure the comfort for the entire space while sufficient ventilation rate does not
 12 guarantee delivery of enough fresh air to breathing zones. Poor ventilation design can lead to
 13 thermal discomfort, draft sensation and lack of fresh air. This paper presents two new
 14 simulation-based air-supply system design methods by comprehensively evaluating and
 15 optimizing space thermal comfort (predicted mean vote – PMV), draft sensation (percent
 16 dissatisfied due to draft – PD), and ventilation effectiveness (age of air). A newly-developed
 17 and validated CFD-based MOGA tool was used for the system designs [7]

18 19 **2. Optimization Method and Design Objective Indices**

20 **2.1 Genetic Algorithm**

21 Genetic algorithm uses evolution operations to transform a population of data objects into a
 22 new population with higher average fitness values [8]. The higher fitness value an individual
 23 have, the closer it is to the optimal result. As one of the gradient-free optimization methods,
 24 GA is capable of resolving nonlinear and multi-solution problems, requiring less computing
 25 time to find global optimal results than other methods [9]. A typical GA procedure breaks
 26 down as follows:

- 27 (1) Generate a random initial population of potential solutions, which contains several
 28 individuals;
- 29 (2) Evaluate the fitness value of each individual with specified cost function (objective);
- 30 (3) Check whether the population meets the prescribed optimization criterion; if not, apply

1 genetic operations such as selection, crossover, and mutation to the population to create a
 2 new generation of potential solutions;
 3 Repeat step (2) and (3) until the optimization criterion is met.
 4 Xue et al. [7] integrated a modified GA with a CFD tool to realize the inverse prediction and
 5 optimization of flow control conditions for confined spaces. Tournament selection method
 6 was adopted for gene selection operation. Individuals crossover at single point for every
 7 variable, which means multi-point-crossover for multi-variable problems. Constant mutation
 8 rate was used. Calculation stops until fitness value of each individual in current population
 9 satisfies lower limit of convergence, when the method is used for multi-solution problems.
 10 This study expands that research to include the MOGA calculation that monitors and
 11 evaluates multiple objectives during the same simulation, which is more efficient than
 12 optimizing the indices separately. [8]

14 2.2 Design Objective Index: PMV

15 PMV is a widely used quantitative thermal comfort evaluation index for indoor thermal
 16 comfort assessment [10]. The PMV equation was developed as below:

$$\begin{aligned}
 \text{PMV} = & (0.303e^{-0.036M} + 0.028) \times \{(M - W) - 3.05 \times 10^{-3} \times [5733 - 6.99(M - W) - p_a] \\
 & - 0.42 \times [(M - W) - 58.15] - 1.7 \times 10^{-5} \times M \times (5867 - p_a) - 0.0014 \times M \times (34 - t_a) \\
 & - 3.96 \times 10^{-8} f_{cl} \times [(t_{cl} + 273)^4 - (\bar{t}_r + 273)^4] - f_{cl} h_c (t_{cl} - t_a)\} \quad (1)
 \end{aligned}$$

18 where

$$\begin{aligned}
 t_{cl} = & 35.7 - 0.028(M - W) - I_{cl} \{3.96 \times 10^{-8} \times f_{cl} \times [(t_{cl} + 273)^4 - (\bar{t}_r + 273)^4] \\
 & + f_{cl} h_c (t_{cl} - t_a)\} \quad (2)
 \end{aligned}$$

$$h_c = \begin{cases} 2.38 \times (t_{cl} - t_a)^{0.25} & 2.38(t_{cl} - t_a)^{0.25} > 12.1\sqrt{V} \\ 12.10\sqrt{V} & 2.38(t_{cl} - t_a)^{0.25} < 12.1\sqrt{V} \end{cases} \quad (3)$$

$$f_{cl} = \begin{cases} 1.00 + 1.290I_{cl} & I_{cl} \leq 0.078m^2 \cdot ^\circ C/W \\ 1.05 + 0.645I_{cl} & I_{cl} > 0.078m^2 \cdot ^\circ C/W \end{cases} \quad (4)$$

22 This study uses the PMV as the main design index to ensure the thermal comfort (i.e., thermal
 23 balance) around the occupant. The average PMV is calculated from the absolute PMV values
 24 at a few monitoring points around the body. The objective function is to reach $|\text{PMV}| < 0.1$.

26 2.3 Design Objective Index: PD

27 PD is percent dissatisfied due to draft. Draft is an undesired local cooling of the human body
 28 caused by air movement. Draft has been identified as one of the most annoying factors during
 29 the cooling. When people sense draft, they often demand higher air temperatures in the space
 30 or even shut down the system. Fanger and Christensen [11] attempted to establish the
 31 percentage of the population feeling draft when exposed to a given mean velocity. Fanger et
 32 al. [12] further investigated the effect of turbulence intensity on sensation of draft. Turbulence
 33 intensity significantly affects draft sensation, as predicted by the following model:

$$\text{PD} = (34 - t_a)(V - 0.05)^{0.62}(0.37V\text{Tu} + 3.14) \quad (5)$$

1 where

$$2 \quad Tu = 100 \frac{V_{sd}}{V} \quad (6)$$

3 In practice, for $V < 0.05 \text{ m/s}$, use $V = 0.05$ in Eq. (5), and for $PD > 100\%$, set $PD = 100\%$.

4 This study monitors the PD values around each person's head and ankle, where is the most
5 sensitive area for draft sensation. The design objective is to control the average PD at
6 monitoring points to be below 15% [13]. Generally, draft sensation increases as inlet velocity
7 increases and thus the PD function limits the supply air velocity.

8

9 **2.4 Design Objective Index: Age of Air**

10 Indoor air quality is greatly influenced by ventilation effectiveness [14]. Among indices such
11 as macro air exchange rate, air change efficiency, local air change efficiency, local ventilation
12 index, purging airflow rate, age of air is mostly used to evaluate the actual "freshness" of air
13 at certain locations in the space [15]. Age of air can be obtained by using tracer gas technique
14 or CFD simulation. CFD solves the following transport equation to calculate age of air
15 [16][17]:

$$16 \quad \frac{\partial}{\partial x}(u\tau) + \frac{\partial}{\partial y}(v\tau) + \frac{\partial}{\partial z}(w\tau) = \frac{\partial}{\partial x}\left(D \frac{\partial \tau}{\partial x}\right) + \frac{\partial}{\partial y}\left(D \frac{\partial \tau}{\partial y}\right) + \frac{\partial}{\partial z}\left(D \frac{\partial \tau}{\partial z}\right) + 1 \quad (7)$$

17 Here D is the sum of the molecular diffusion coefficient and the turbulent diffusivity of air.
18 This study predicts and monitors the age of air at each occupant's breathing zone. ASHRAE
19 Handbook [13] requires that the ventilation rate for a person in office must be greater than 8
20 L/s. Assuming a person occupies 2 m^3 space, the largest age of air would be about 250s and
21 the average age of air would be less than 125s. The design objective for age of air is set as
22 being less than 125s for better air quality. Generally, decrease in inlet ventilation rate leads to
23 the increase of age of air, and hence using age of air will assist setting a lower limit on
24 ventilation rate. Since energy use of a HVAC system is a function of supply air flow rate and
25 temperature, which are reflected by PMV, PD and age of air directly or indirectly. Energy
26 consumption of a system thus is not specified directly as an optimization objective, which
27 however will be considered when selecting a final optimal solution.

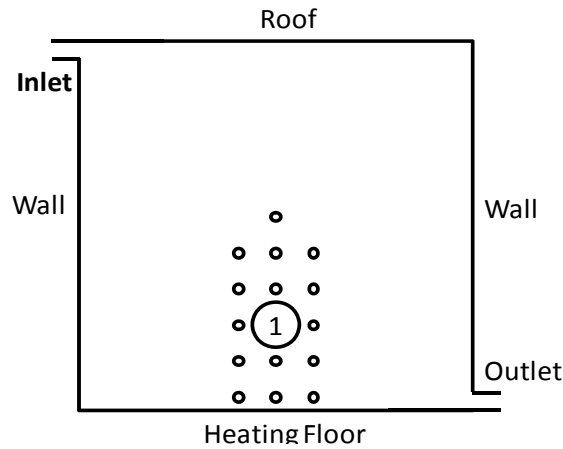
28

29 **3. Methodologies – 2-D Office Case**

30 The study uses a 2-D mixing convection case [18] to evaluate the proposed ventilation system
31 design methods. The case is a widely used with representative indoor flow mechanisms of
32 natural convection (floor heating) and forced convection (mechanical ventilation system). The
33 case has a clear definition of geometries and boundary conditions, which is ideal for assessing
34 new methods and models for indoor environment applications.

35 Experimental results were obtained from the literature, which were measured in a laboratory
36 chamber of $1.04 \text{ m} \times 1.04 \text{ m} \times 0.7 \text{ m}$ ($x \times y \times z$) equipped with a 18mm wide inlet slot and a 24mm
37 wide outlet slot. The experiment produced a fairly good 2-D flow at the central plane. The
38 flow at the central plane can thus be simulated using a 2-D CFD model (shown in Fig. 1). The
39 experiment measured the wall temperatures and supply air conditions, respectively, as $T_{\text{roof}} =$
40 $T_{\text{walls}} = 15^\circ \text{C}$, $T_{\text{floor}} = 35.5^\circ \text{C}$, $T_{\text{inlet}} = 15^\circ \text{C}$, $V_{\text{inlet}} = 0.57 \text{ m/s}$ (normal to the inlet slot), as well as

1 temperature, x-velocity magnitude and y-velocity magnitude at the ten points along the
 2 middle line on the central plane. The turbulent kinetic energy and turbulent dissipation rate of
 3 the inlet were controlled to be $0.00125\text{m}^2\text{s}^{-2}$ and 0.



4
 5 Fig. 1 CFD model of the 2-D office case
 6

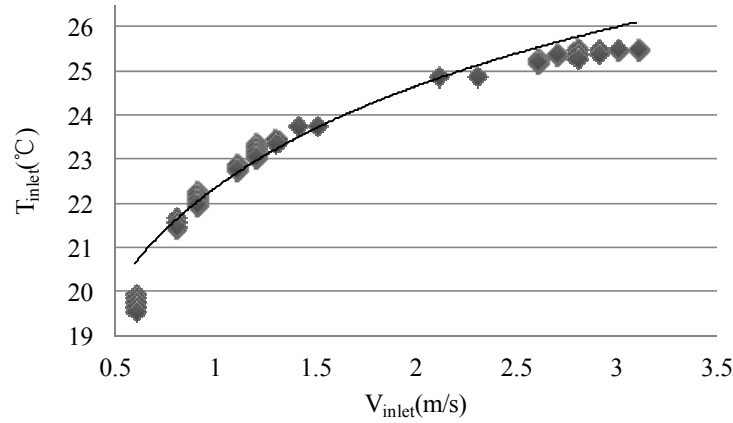
7 The study uses Fluent of Ansys 12.1 to solve the velocity and temperature field. The RNG k- ϵ
 8 model is used for its good performance in indoor environment simulation. The Boussinesq
 9 assumption is adopted to simulate natural convection. The study first used the experiment data
 10 to verify the simulation model. The validated model is used for inlet supply parameters design.
 11 The design goal is to optimize the inlet supply parameters that achieve good indoor
 12 environment quality. The parameters to be optimized include: inlet air temperature (T_{inlet} :
 13 between 10-30 °C), inlet air velocity magnitude (V_{inlet} : between 0-5 m/s). Because the size of
 14 inlet and the flow direction are fixed, change of velocity magnitude implies the change of
 15 ventilation rate. The optimization goals are, for Zone 1 (in Fig. 1), $|\text{PMV}| < 0.1$, $\text{PD} < 15\%$ and
 16 age of air $< 125\text{s}$. Mean value of the 16 points distributed in Zone 1 is used to represent the
 17 overall conditions of the zone. Number of individuals in the population is 8, crossover rate is
 18 0.8 and mutation rate is 0.1.

19 3.1 The Constraint Method

20 The constraint method focuses on one main index while using the other indices to constrain
 21 the applicable range of parameters. The main index in this study is $|\text{PMV}| < 0.1$ for Zone 1. It
 22 requires about 20 generations to converge. Figure 2 shows the identified solutions with
 23 different combinations of supply air temperature and velocity magnitude that can all meet the
 24 PMV requirement in Zone 1. The supply air velocity magnitude and temperature demonstrate
 25 a following logarithmic relationship:

$$26 \quad T_{\text{inlet}} = 3.3202\ln(V_{\text{inlet}}) + 22.344 \quad (8)$$

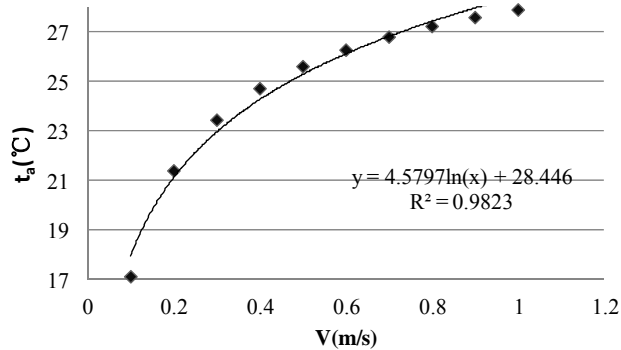
27



1
2 Fig. 2 Logarithmic relationship between inlet velocity and temperature for $|\text{PMV}| < 0.1$ in Zone
3 1

4
5 Analysis of Eq. (1) shows a similar relationship between t_a and V . Assuming $M=65 \text{ Wm}^{-2}$ (the
6 general value of slight labor intensity), $W=0 \text{ W}$ (sedentary person without mechanical work),
7 $p_a=10\text{kPa}$, $I_{cl}=0.1 \text{ clo}$, and \bar{t}_r equals air temperature near walls, when PMV is set to zero, the
8 following logarithmic relationship is observed from Eq. (1):

$$9 \quad t_a = 4.5797 \times \ln(V) + 28.446 \quad (9)$$



11
12 Fig.3 Logarithmic relationship between inlet velocity and temperature for $\text{PMV}=0$ from the
13 PMV equation

14
15 Equations (8) and (9) share a similar expression as:

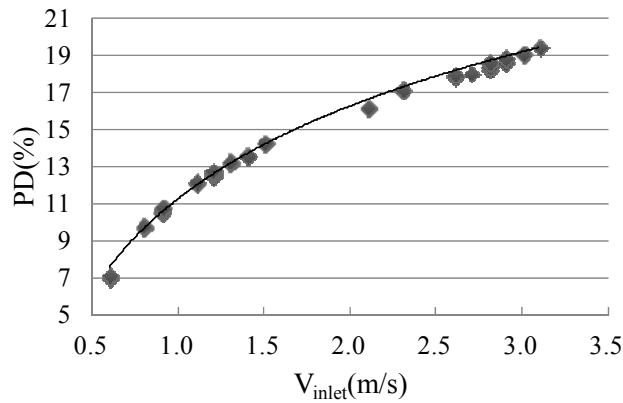
$$16 \quad y = A \times \ln(x) + B \quad (10)$$

17 This analysis reveals that the inherent mathematic relationships among the parameters in the
18 cost function can affect (and even determine) the relationships among the parameters at the
19 boundary. If the correlation format of the input variables can be pre-determined (e.g., Eq.
20 (10)), theoretically, only few points (e.g., two points – two optimal cases – for this case) are
21 needed to determine the coefficients (e.g., A and B for Equation (10)) so that the entire pool
22 of potential optimal cases (e.g., the curve in Fig 2) can be determined. This can significantly
23 reduce the optimization simulation effort in CFD-GA.

24 For all the points identified in Fig. (2), their PD and age of air values in Zone 1 were
25 calculated and recorded. The results show that both PD and age of air have a strong

1 relationship with inlet flow velocity as shown in Fig. 4 and Fig. 5, respectively, but less
 2 dependent on supply air temperature.

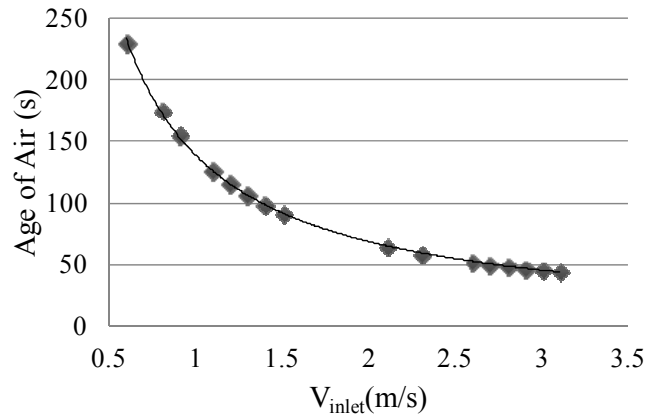
3



4

5 Fig. 4 Relationship between inlet flow velocity and PD in Zone 1

6



7

8 Fig. 5 Relationship between inlet flow velocity and age of air in Zone 1

9

10 The regression equation of the curve in Fig. 4 is:

11
$$PD(\%) = 7.2169 \times \ln(V_{inlet}) + 11.256 \quad (11)$$

12 And the regression equation of the curve in Fig. 5 is:

13
$$\text{Age of Air} = 139.09 \times V_{inlet}^{-1.02} \quad (12)$$

14

15 For PD = 15%, the inlet flow velocity is 1.67 m/s according to Eq. (11), and the age of air will
 16 be 82 s according to Eq. (12). This provides the upper limit of the supply velocity. For age of
 17 air = 125s, the inlet flow velocity will be 1.11 m/s according to Eq. (12), and the PD will be
 18 12% according to Eq. (11). This provides the lower limit of the supply velocity. Applying
 19 both constraints to the curve in Fig. 2. produce the suitable range of input variables that can
 20 meet all the three objective indices, as showed by the red line between P1 (1.11 m/s, 22.69°C)
 21 and P2 (1.67 m/s, 24.05°C) in Fig. 6.

22

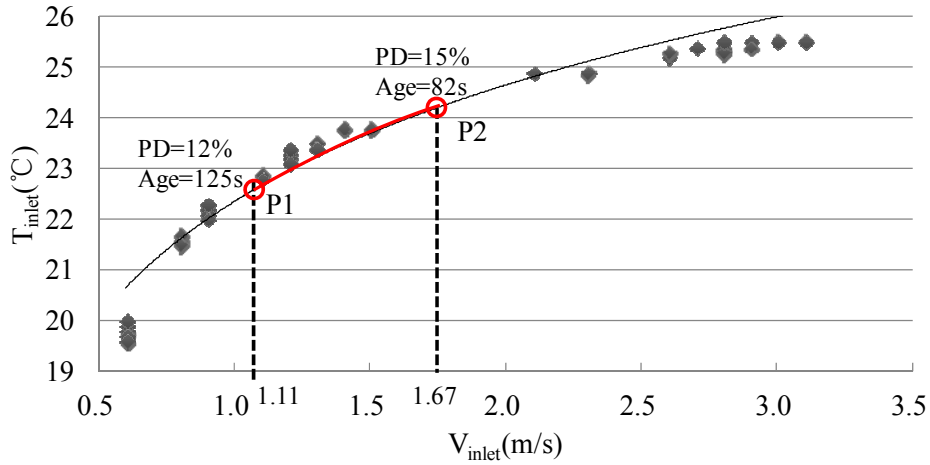


Fig. 6 Optimal cases identified by the constraint method

3.2 The Optimization Method

The multi-objective GA method, along with CFD, is also applied to optimize the design using the three indices simultaneously. Fundamentally, three CFD-GA simulations were performed, using the three objective functions (PMV, PD, and age of air), respectively. It requires more than 30 generations to converge. The applicable ranges of supply parameters from each simulation were then plot on the same figure to find the final optimal cases that meet all the design criteria.

Similar to the PMV results in Fig. 2, the PD simulation also identifies a set of possible solutions with different combinations of supply air temperature and velocity magnitude that can meet the PD requirement in Zone 1 (i.e., the average PD of Zone 1 equals 15%). In Fig. 7, every point at upper left of the curve satisfies the requirement that $PD < 15\%$ in Zone 1. This curve thus provides a boundary of acceptable supply air velocity and temperature for PD consideration.

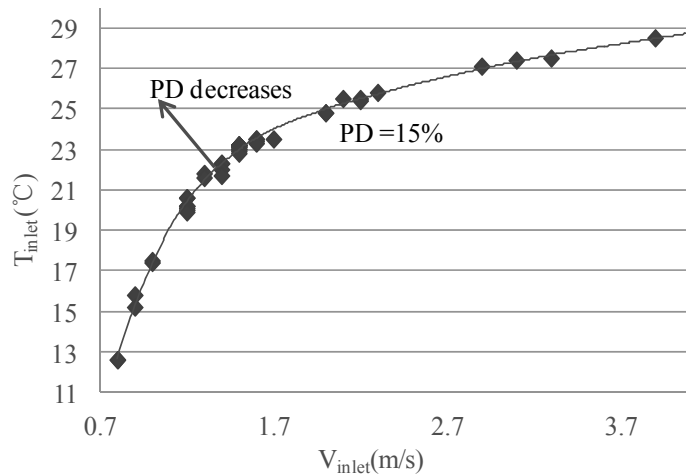
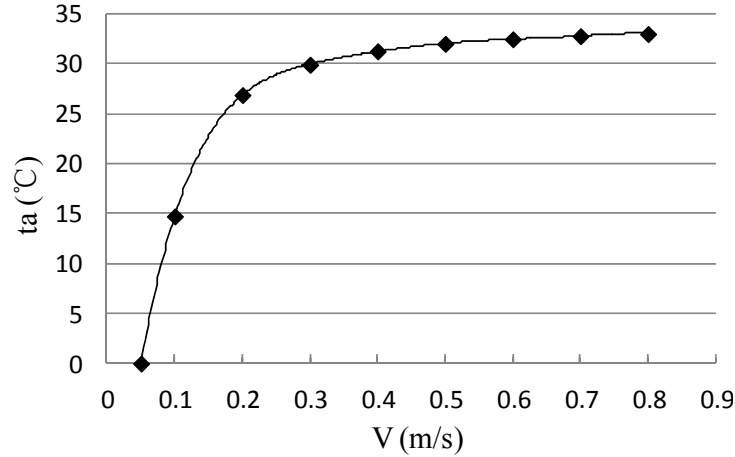


Fig. 7 Relationship between inlet flow velocity and temperature satisfying $PD=15\%$ in Zone 1



1

2 Fig. 8 Correlation between air velocity and temperature for PD = 15% from the PD equation

3

4 Similar approach as the earlier PMV simulation can be used to reduce the number of cases
 5 required to produce the PD curve in Fig. 7, by using a pre-defined expression between air
 6 velocity and temperature. This pre-defined expression is obtained by analyzing the PD Eq. (5),
 7 as shown in Fig. 8 where Tu = 50 and PD = 15% (the set upper limit), which reveals a similar
 8 trend as the curve in Fig. 7. A six-order polynomial can be applied to fit the curve in Fig. 8,

9

$$\begin{aligned}
 ta = & -3368.9V^6 + 10572V^5 - 13495V^4 + 8987V^3 \\
 & - 3317.5V^2 + 658.94V - 25.701
 \end{aligned}
 \tag{13}$$

10

11 To predict the curve in Fig. 7 using the pre-defined six-order polynomial expression, therefore,
 12 requires only six cases (points) to identify the six coefficients that are below:

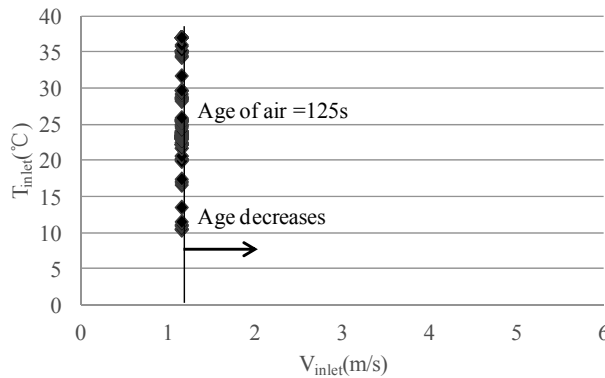
13

$$\begin{aligned}
 T_{inlet} = & -0.0733V_{inlet}^6 + 1.403 V_{inlet}^5 - 10.993 V_{inlet}^4 + 45.156 V_{inlet}^3 \\
 & - 103.05 V_{inlet}^2 + 126.69 V_{inlet} - 41.753
 \end{aligned}
 \tag{14}$$

14

15 The simulation results do not reveal an explicit relationship between the age of air and supply
 16 air temperature. Rather, the age of air is dominantly influenced by the supply air flow rate (i.e.,
 17 velocity) as presented in Fig. 9. The study shows that the supply flow velocity must be larger
 18 than 1.15 m/s to ensure an average age of air of less than 125s in Zone 1.

19



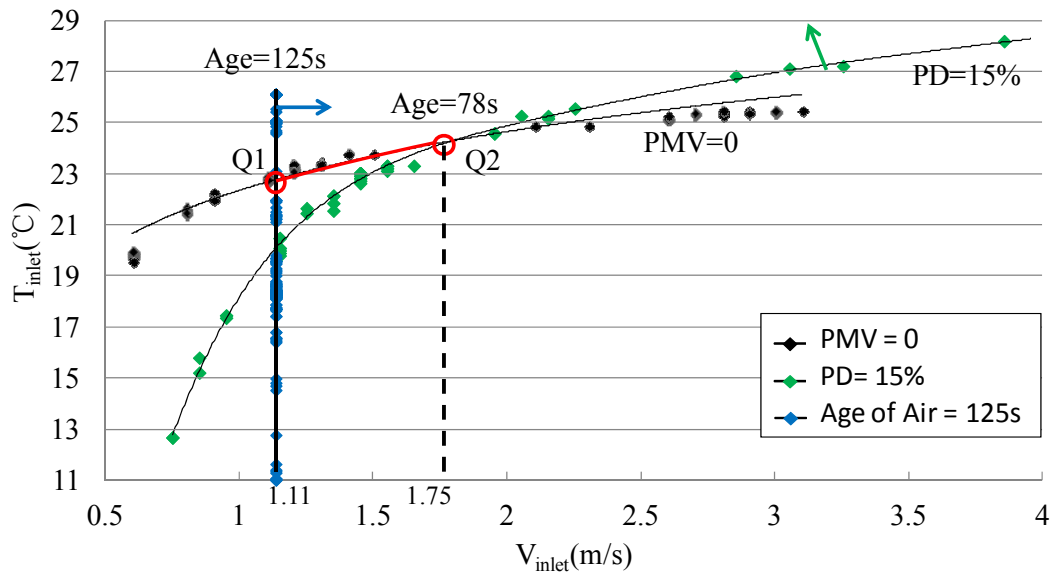
20

21 Fig. 9 Correlation between supply air velocity and temperature for age of air = 125s in Zone 1

22

23 To identify optimal design parameters that can achieve multiple design objectives, the three

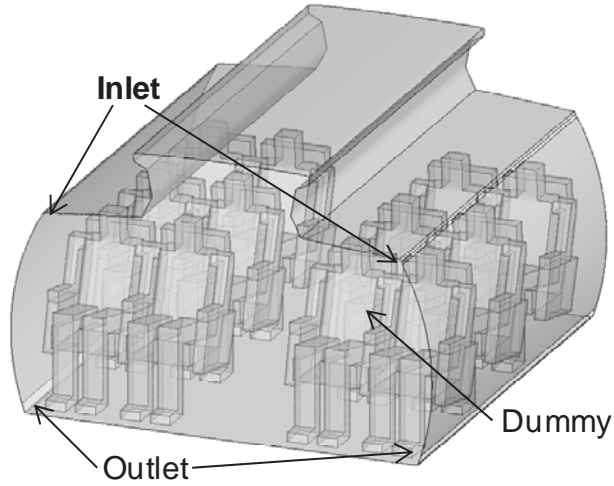
1 optimal curves from Fig. 7-9 are then assembled into one figure as seen in Fig. 10. All points
 2 on the curve of PMV=0 ensure the thermal comfort in Zone 1. The curve of age of air=125s
 3 intersects with the curve of PMV=0 at Q1 (i.e., 1.11m/s, 22.69°C). When supply velocity is
 4 greater than 1.11m/s, the average age of air in Zone 1 will be below 125s. So Q1 is the lower
 5 limit point. The PMV=0 curve and the PD= 15% curve intersect at point Q2 (1.75m/s, 24.2°C).
 6 Simulation results show that points located at upper left of the curve PD=15% can deliver
 7 lower draft sensation in Zone 1. Hence Q2 provides the upper limit of the acceptable supply
 8 air velocity. Only the points on the red line in Fig. 9 can meet all the three design criteria,
 9 showing a very similar but slightly larger range than those from the constraint method, the red
 10 line between P1 (1.11 m/s, 22.69°C) and P2 (1.67 m/s, 24.05°C) in Fig. 6.
 11



12
 13 Fig. 10 Optimal cases identified by the multi-objective optimization method
 14

15 4. Demonstration – 3-D Aircraft Cabin Case

16 The study employed the developed method to optimize supply air conditions in an aircraft
 17 cabin. A 3-D aircraft cabin, shown in Fig. 11, was modeled with actual geometries and supply
 18 and return air locations. The cabin had three rows of seats, all occupied by heated dummies of
 19 75W each. During the cruise in the summer, the outside surface temperature of aircraft is
 20 around -46.8°C. The thickness of aircraft wall thermal insulation material is known at
 21 0.0762m, with a thermal resistance of 0.035Wm⁻¹K⁻¹. The heat transfer coefficient at the cabin
 22 exterior surface is about 100W m⁻²K⁻¹. Environment Control System (ECS) of aircraft
 23 typically use 50% return air for ventilation. Thus, the age of air was replaced by the total age
 24 of air [19] as the index of indoor air quality, which takes into account the age of the supply air.
 25 In this study, the allowed inlet parameter ranges were set as: 0.6-2.7 m/s for V_{inlet}
 26 (corresponding ventilation rate of 6-11h⁻¹) and 11-25°C for T_{inlet}. The study goal was to find
 27 optimal inlet parameters that can produce a comfortable and healthful environment around the
 28 occupants (i.e., the dummies). The same design objective functions and parameter setting as
 29 for the 2-D office case were adopted for this study. It requires around 20 generations for the
 30 constraint method and 40 generations for the optimization method to converge.

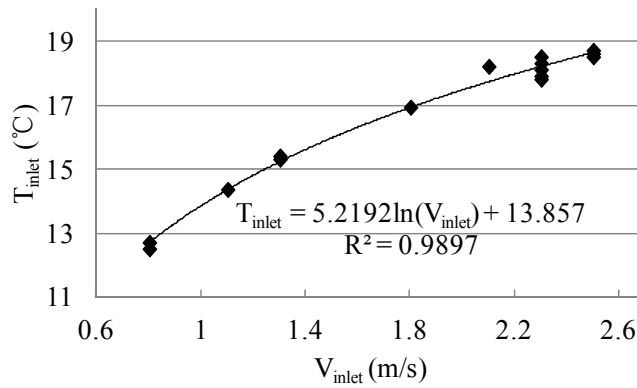


1
2
3
4
5
6
7

Fig. 11 The 3-D aircraft cabin model

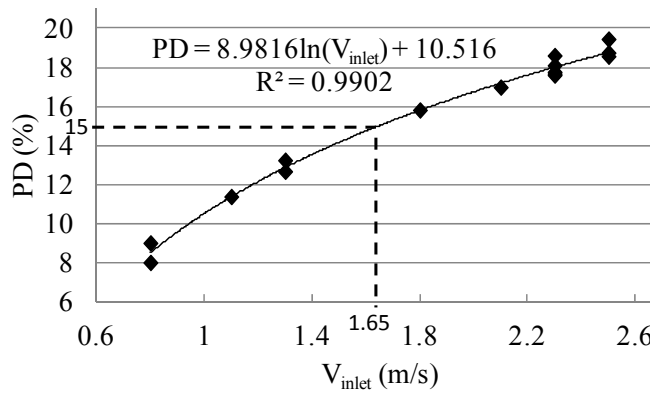
4.1 Results from the Constraint Method

Figure 12 shows the optimal PMV=0 curve in the 3-D aircraft cabin. The predicted relationships of PD and age of air in the monitored zone with inlet flow velocity, respectively, are presented in Fig. 13 and Fig. 14.



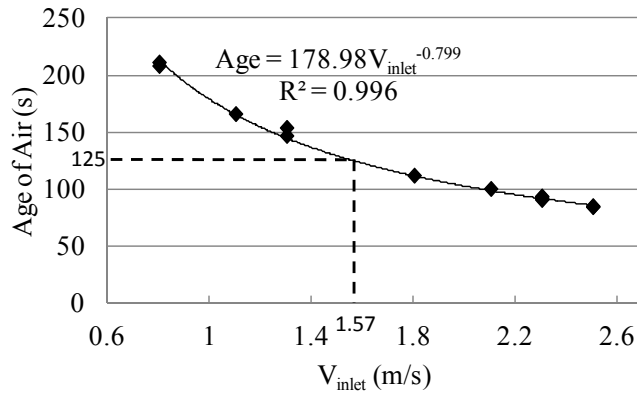
8
9
10

Fig. 12 Curve of PMV= 0 for the 3-D aircraft cabin case



11
12
13

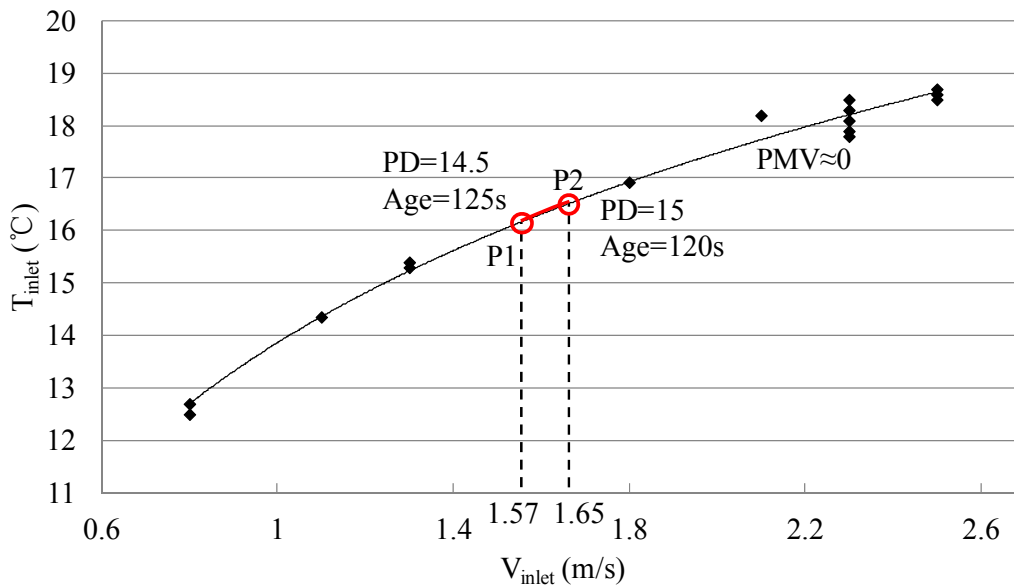
Fig. 13 Relationship between PD and inlet flow velocity for the 3-D aircraft cabin case



1
2 Fig. 14 Relationship between age of air and inlet flow velocity for the 3-D aircraft cabin case

3
4 The regression equations of the three curves are provided in the figures. Following the
5 procedure of the constraint method, the study identifies the optimal inlet flow parameters as
6 shown on the red line between lower limit P1 (1.57m/s, 16.2°C) and upper limit P2 (1.65m/s,
7 16.5°C) in Fig. 15.

8



9
10 Fig. 15 Optimal inlet parameters of the 3-D aircraft cabin case from the constraint method

11

12 4.2 Results from the Optimization Method

13 Figure 16-18 present the optimal curves for PMV = 0, PD =15% and age of air = 125 s using
14 the multi-objective optimization method with a total 179 simulation cases. The regression
15 equations of these curves are again shown in the figures. The red line between lower limit Q1
16 (1.5 m/s, 15.9°C) and upper limit Q2 (1.72 m/s, 16.7°C) in Fig. 19 is identified as the optimal
17 inlet solutions for the air cabin, which is very similar to that obtained from the constraint
18 method, the red line between P1 (1.57m/s, 16.2°C) and P2 (1.65m/s, 16.5°C) in Fig. 15. The
19 study chose a few points on this red line to double check the PMV, PD and age of air statuses
20 under these supply conditions and confirmed all of them can satisfy the prescribed design

1 criteria (and thus verified the viability and effectiveness of the developed method).

2

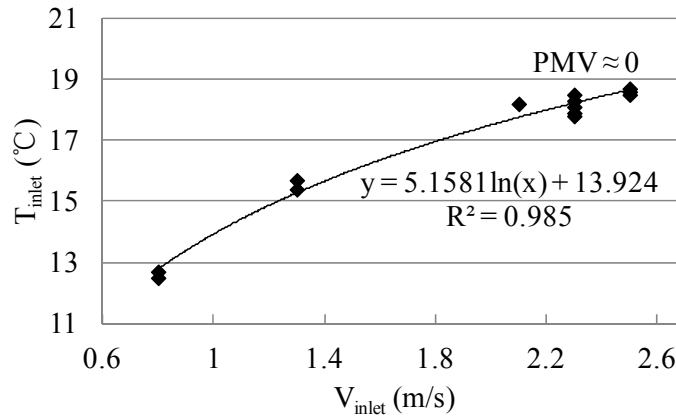


Fig. 16 Relationship between supply air velocity and temperature for PMV = 0

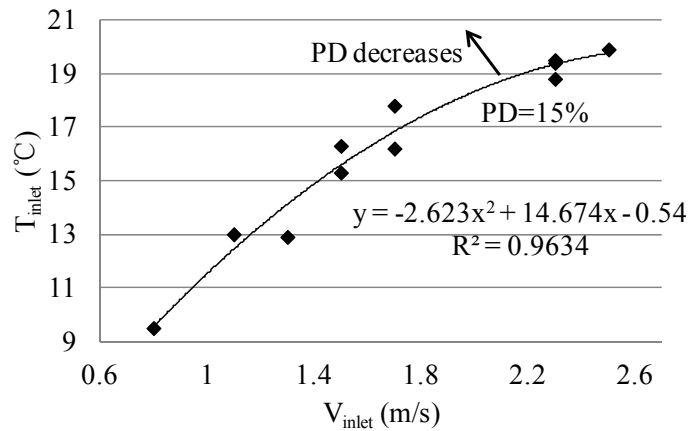


Fig. 17 Relationship between supply air velocity and temperature for PD=15%

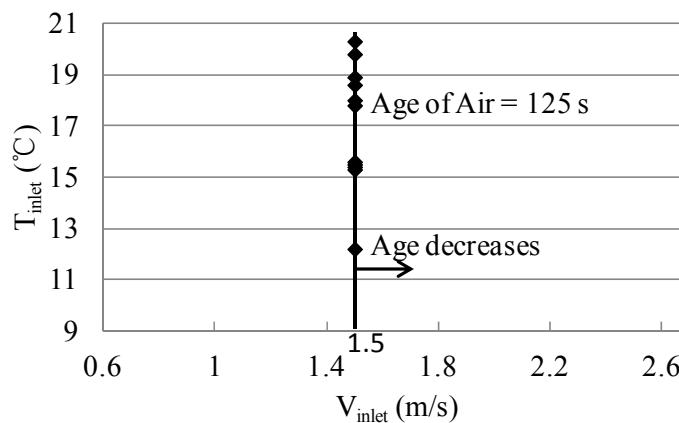


Fig. 18 Relationship between supply air velocity and temperature for age of air = 125s

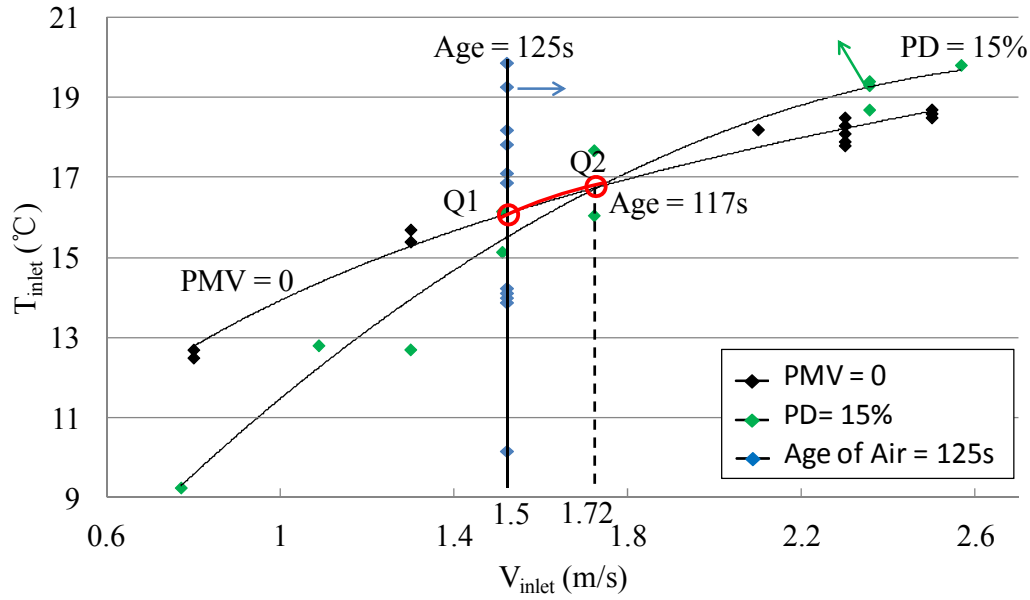


Fig. 19 Optimal inlet parameters of the 3-D aircraft cabin case from the multi-objective optimization method

It is noticed that suggested inlet flow parameters using the traditional calculation method, which only considers thermal balance and ventilation rate requirement of the whole cabin, were 1.3 m/s for supply air velocity and 19°C for supply air temperature. Age of air in breathing area is 145s (calculated based on the equation in Fig 14). It is explicit that design with such parameters may lead to hot and stuffy air around the passengers.

5. Discussions and Conclusions

This study developed a CFD-based MOGA simulation program that can be used to predict and optimize flow control conditions satisfying multiple design indices in various confined spaces. Primary indoor environment quality indicators including PMV, PD and age of air are applied to design a comfortable and healthful indoor environment. The study proposed two system design/optimization methods: the constraint method and the optimization method. Both of them show superior performance than the conventional approach.

The constraint method requires less calculation effort than the optimization method, while the multi-objective optimization approach is somehow more inclusive with less assumptions. Both methods provide similar results, as evidenced by the very-close final ranges of the optimal inlet parameters. As a result, the constraint method may be suggested for most practical applications.

The analysis shows that supply air temperature has small influence on the age of air for the cases studied mainly due to the strong force convection features in these cases. As a result, for similar cases, the age of air can be optimized only on supply air velocity (or flow rate), which can largely reduce the simulation effort for the multi-objective optimization method.

Other flow control parameters such as vent location, flow direction, vent size will have important influence on the design criteria, and indeed can be incorporated into the developed algorithm. The results of these studies will be presented in a separate paper. Please note that

1 all the curves and equations presented in this paper are based on a fixed and specific vent
2 location, flow direction and vent size.

3 4 **6. Acknowledgments**

5 This project was supported by the National Basic Research Program of China (The 973
6 Program of China) through grant No. 2012CB720100. The authors are also grateful for the
7 assistances received from Luyi Xu and Lu An at Tianjin University.

8 9 **References**

- 10 [1] Huang, W. and Lam, H.N.(1997) Using genetic algorithms to optimize controller
11 parameters for HVAC systems, *Energy and Buildings*, 26(3), 277-282
- 12 [2] Wright, J.A., Loosemore, H.A.and Farmani, R. (2002) Optimization of building thermal
13 design and control by multi-criterion genetic algorithm, *Energy and Buildings*, 34(9),
14 959-972
- 15 [3] Fong, K.F., Hanby, V.I. and Chow, T.T. (2006) HVAC system optimization for energy
16 management by evolutionary programming, *Energy and Buildings*, 38(3), 220-231
- 17 [4] Zhou, L. and Haghghat, F. (2009) Optimization of ventilation system design and
18 operation in office environment, Part I: Methodology, *Building and Environment*, 44(4),
19 651-656
- 20 [5] Zhou, L. and Haghghat, F. (2009) Optimization of ventilation systems in office
21 environment, Part II: Results and discussions, *Building and Environment*, 44(4), 657-665
- 22 [6] Boithias, F., Mankibi, M.E. and Michel, P. (2012). Genetic algorithms based optimization
23 of artificial neural network architecture for buildings' indoor discomfort and energy
24 consumption prediction , *Building Simulation: an International Journal*, 5, 95-106
- 25 [7] Xue, Y., Zhai, Z.J. and Chen, Q. (2013) Inverse prediction and optimization of flow
26 control conditions for confined spaces using a CFD-based genetic algorithm, *Building and
27 Environment*, 64, 77-84
- 28 [8] Koza, J. R. (1992) *Genetic Programming: On The Programming of Computers By Means
29 of Natural Selection*, Cambridge, Massachusetts Institute of Technology Press.
- 30 [9] Sakamoto, Y., Nagaiwa, A., Kobayasi, S. and Shinozaki, T. (1999) An optimization
31 method of district heating and cooling plant operation based on genetic algorithm,
32 *ASHRAE Transactions*, 105(2), 104-115.
- 33 [10] Fanger, P.O. (1970) *Thermal Comfort, Analysis and Applications in Environmental
34 Engineering*, Copenhagen, Danish Technical Press.
- 35 [11] Fanger, P.O. and N.K. Christensen (1986) Perception of draught in ventilated spaces,
36 *Ergonomics*, 29(2), 215-235.
- 37 [12] Fanger, P.O., Melikov, A.K., Hanzawa, H. and Ring, J. (1989). Turbulence and draft,
38 *ASHRAE Journal*, 31(4), 18-25.
- 39 [13] ASHRAE (2011) *ASHRAW Handbook-HVAC Applications(SI)*, Atlanta GA, American
40 Society of Heating, Refrigerating and Air Conditioning Engineers.
- 41 [14] Hedge A. (1996) Predicting sick building syndrome at the individual and aggregate
42 levels, *Environment International*, 22(1), 3-19
- 43 [15] Sandberg M, Sjoberg M. (1983) The use of moments for assessing air quality in
44 ventilated rooms, *Building and Environment*, 18(4), 181-97

- 1 [16] Kato S, Murakami S. (1988) New ventilation efficiency scales based on spatial
2 distribution of contaminant concentration aided by numerical simulation. *ASHRAE*
3 *Transactions*, 94(2), 309–30
- 4 [17] Etheridge, D. and Sandberg, M. (1996) *Building Ventilation: Theory and Measurement*,
5 *John Wiley & Sons, Chichester*
- 6 [18] Blay, D., Mergui, S. and Niculae, C. (1992) Confined turbulent mixed convection in the
7 presence of a horizontal buoyant wall jet, *Fundamentals of Mixed Convection*, 213,
8 65–72.
- 9 [19] Li, X., Li, D., Yang, X. and Yang, J. (2003) Total air age: An extension of the air age
10 concept, *Building and Environment*, 38(11), 1263-1269